

## Modelling of turbulent flow transients within Hot Dry Rock fracture systems: Preliminary results

T. Kohl<sup>1</sup>, K.F. Evans<sup>1</sup>, R.J. Hopkirk<sup>2</sup>, R. Jung<sup>3</sup> and L. Rybach<sup>1</sup>

<sup>1</sup> Institut für Geophysik, ETH-Honggerberg, CH-8093 Zurich, Switzerland

<sup>2</sup> Polydynamics Ltd., Zeltweg 16, CH-8032 Zurich, Switzerland

<sup>3</sup> Bundesanstalt für Geowissenschaften und Rohstoffe, Stilleweg 2, D-30631 Hannover, Germany

key words: forced fluid flow, fractured rock, hydraulic testing, non-laminar flow model

### Abstract

During the HDR site investigation studies in Soultz s.F. (France) stepwise hydraulic injection and production tests have been conducted in the borehole GPK1. The datasets that were obtained from the lowermost depth domain between 2850 m and 3490 m demonstrate non-laminar hydraulic behaviour. At near steady state conditions changes in flow rate invoke parabolic pressure changes. This observation together with earlier datasets from the same site are corresponding to empirical flow laws established for turbulent hydraulic regimes. As a consequence from this non-linearity, conventional hydrological models cannot be used to interpret these hydraulic tests.

In this paper we describe a model which permits non-laminar flow in fractures that is being developed for this purpose. As a first exercise, the model has been applied to the injection test at GPK1. The results show that certain features of the observed transient response which cannot be explained by a conventional laminar flow model are predicted by the non-linear flow law. A preliminary evaluation of the parameters resulting from both, steady state and transient analysis leads to assumptions on the geometry of the main fracture system. Depending on the assumption for the surrounding matrix, our calculations provide the basis for a large surface area of the fracture.

### Introduction

The European Hot Dry Rock (HDR) investigation site Soultz s.F. is situated in the middle part of the Upper Rhine Valley, 50 km north of Strasbourg where surface heat flow attains values above  $0.150 \text{ W m}^{-2}$ . At greater depth, the heat flow reduces and stabilises below the crystalline basement at 1400 m depth at values around  $0.09 \text{ W m}^{-2}$ . The area at Soultz is transversed by several large scale N-S striking fault zones. The maximum horizontal stress component is directed approximately N170°E and its magnitude is believed to be similar to the vertical stress. The minimum horizontal stress is only about half as large and is about 10 MPa above hydrostatic water pressure.

A 3.6 km deep borehole, GPK1, has been drilled 2 km into the crystalline basement and is intended to be the production leg of a duplet system. The well has been cased to 2850 m, some 1450 m below the top of the basement.

Hydraulic tests with different flow or pressure steps were performed during 1994 in the open hole section of GPK1. They showed a clear evidence that non-laminar, turbulent-like flow was occurring somewhere within the reservoir fracture system (Jung and Schellschmidt, 1994, Jung *et al.*, 1995). The same behaviour was observed in similar tests conducted on the same hole section prior to stimulation, and also in tests that followed modest stimulation injections into a shallower zone near 1985 m during an earlier testing phase of GPK1 (Jung, 1992b).

Up to now, the interpretation of hydraulic datasets from the Soultz HDR site was restricted to laminar flow assumptions. Since one step hydraulic injection data do not demonstrate the necessity for non-laminar flow analysis, interpretations based on laminar flow conditions could be performed for the hydraulic experiments at Soultz. Jung (1990) fitted the beginning of the one step stimulation curve during which a fracture, intersecting GPK1 at a depth range of 1968–2000 m (88DEC13) was stimulated. He derived parameters of storativity and hydraulic conductivity of matrix and fracture by using the analytical, laminar flow formulations by Cinco & Samaniego (1981). Kohl (1992) then succeeded in fitting the total

of the stimulation test 88DEC13 with the Finite Element (FE) code FRACTure assuming laminar fracture flow. Also, laminar flow conditions were presumed by Bruel & Ezzedine (1994) who investigated a subsequent stimulation test in the same depth domain of GPK1. They fitted the pre- and post-stimulation pressure response using coupled hydro-mechanical algorithms with a discrete fracture distribution.

Despite the evident importance of non-laminar flow for the development of the Soultz reservoir, there has been no detailed systematic study of the nature of the problem. In part this is due to the absence of a flexible model that allows the effects of various non-laminar flow laws and fracture flow geometries on well-reservoir impedance to be examined. Currently, only data pertaining to the steady-state condition have been quantitatively analysed, whereas the transient curves undoubtedly contain useful information about the reservoir. To provide a tool for extracting such information, a finite element code, FRACTure, is being extended to include turbulent-like flow within fractures (Kohl *et al.*, 1992; Kohl and Hopkirk, 1995). At the present stage of development, a simple 2D model has been set-up and applied to the 1994 injection test series. Specifically, we focus on the uppermost 50 m of the open hole section below the casing shoe where 60% of the flow entered the formation, and attempt to reproduce the differential pressure changes that accompanied the flow-rate steps.

### Background to deep hydraulic tests in GPK1

During 1993 the open hole section of GPK1 (2850–3600 m) was subjected to a series of major stimulation injections during which a net volume of 40000 m<sup>3</sup> of fresh water was injected. During these tests, injection rate was stepped through 11 levels from  $0.15 \text{ l s}^{-1}$  to  $50 \text{ l s}^{-1}$  (Jung *et al.*, 1995). Wellhead pressure initially increased significantly in response to flow-rate steps, reaching 8 MPa for the  $6 \text{ l s}^{-1}$  level, but subsequently stabilised at 10 MPa for the higher flow rates, indicating that jacking (i.e. fracture dilation) was occurring. Spinner logs run during the highest rate injections at the end of the sequence indicated that 60% of the injected water entered the formation over the 50 m hole section that lay immediately below the casing shoe.

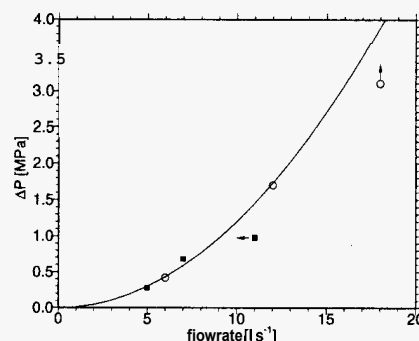


Figure 1: Plot of 'steady-state' downhole differential pressure,  $\Delta P$ , versus flow rate for all steps in the production (squares) and injection (circles) tests conducted on the entire open hole section of GPK1 during 1994. The arrows indicate the direction of the transient. The parabolic curve corresponds to the best-fit prediction of a fully-turbulent system (see also Jung *et al.*, 1995).

The success of the stimulations in linking the borehole to the reservoir was evaluated in 1994 when a production (94JUN16) and injection test (94JUL04) were conducted. In each test, flow-rate was held constant until steady-state conditions were approached, after which it was stepped to a new level. In the 94JUN16 experiment, production flow rates of 5, 7 and 11 l s<sup>-1</sup> were encountered. Injection flow rates of 6, 12 and 18 l s<sup>-1</sup> were used during the 94JUL04 test. Spinner logs showed the same flow profile as prevailed towards the end of the stimulation injections, with 60% of the net flow entering or leaving the formation over the 50 m section below the casing shoe. The pressure that 'drives' flow in these tests is the difference between the measured downhole pressure and the natural formation pressure, and we will refer to this as the downhole differential pressure,  $\Delta P$ . This pressure remained at least 5 MPa below that required for jacking throughout the tests. The plot of steady-state  $\Delta P$  against flow rate for each step in these tests is shown in Figure 1. The relation is clearly not linear, as would be expected for Darcy flow, but rather has the form expected for a fully-turbulent system in which  $\Delta P$  varies with the square of flow rate,  $Q^2$  (Jung and Schellschmidt, 1994; Jung et al., 1995). This suggests that non-laminar flow may be a common facet of fracture flow at moderate to high flow rates within the Soutz, and perhaps other HDR reservoirs. For GPK1, the implication of this behaviour is that drawdowns of the order of 4 MPa below natural formation pressure will be required to attain production of 20 l s<sup>-1</sup> unless reservoir pressures in the near field of GPK1 become elevated as a consequence of injection into GPK2, the other well in the duplet (i.e. a closed circulation system is established).

The transient dataset of the 94JUL04 test that will be considered by the present paper can be recognised in Figure 2. Important characteristics of this curve are that it takes days to approach steady-state levels and that this period increases with higher flow rate and pressure (1.4E05 s, 2.4E05 s and 7.8E05 s, resp.).

### 1D Empirical Turbulent Flow Laws

By means of the Reynolds number ( $Re$ ) the onset of a turbulent flow regime can be described. The Reynolds number for flow between parallel plates, is given by

$$Re = \frac{2\rho q}{\mu} \quad (1)$$

where  $\rho$ ,  $q$  and  $\mu$  are the density of the fluid, the flow rate per unit fracture height and the dynamic viscosity of the fluid, respectively. Eqn.1 shows that at a given flow rate, the Reynolds number is independent of the fracture aperture. It is generally considered that turbulent flow in pipes requires  $Re > 2200$  (Turcotte & Schubert, 1982). Taken the typical values for water at 100°C (density

970 kg m<sup>-3</sup> and viscosity  $3 \times 10^{-4}$  Pa s)  $q$  has to be greater than 0.35 l s<sup>-1</sup>. To increase the Reynolds number to 2200 would require the flow of the smallest injection rate of 94JUL04 which enters the formation over the topmost 50 m in the open hole section to be funnelled through a fracture of a maximum height of 10 m.

A second explanation for the turbulent observations of 94JUL04 is that turbulence begins at much lower parallel-plate Reynolds numbers for fractures in intimate contact. This conclusion is supported by Lomize (1951) whose experiments are extended and reported by Louis (1967). They demonstrate that the onset of turbulence depends upon the relative roughness  $WD$ . This value describes the height of asperities over the mean aperture. Values close to zero represent smooth fractures, whereas values up to 0.4 represent rough fracture surfaces (Evans et al., 1992). According to Louis (1967) these high roughness may cause turbulence already at  $Re \approx 100$ . Applying this value to the 94JUL04 experiment, turbulent flow is imposed even at fracture heights of 200 m.

Since the studies of Lomize (1951), Louis (1967) and Sharp (1970) give evidence to suggest that Reynolds Numbers calculated for flow between parallel-plates are not appropriate for characterising the flow regime in fractures in intimate contact in the present paper Reynolds Number considerations are ignored.

Louis (1967) reported and established different empirical non-laminar flow laws, which apply for fractures at different relative roughnesses. One-dimensional, fully-turbulent flow through smooth fracture surfaces ( $k/D_h = 0.0$ ) is described by the Blasius law, through rougher surfaces (up to  $k/D_h < 0.032$ ) by the Nikuradse law and through very rough surfaces ( $k/D_h > 0.032$ ) by the Louis law. In the present analysis, the Nikuradse law was applied. In contrast to the linear relation between the flow velocity  $v$  and the pressure gradient  $\nabla P$  appropriate the laminar Darcy law

$$v = -K \cdot \nabla P \quad (2)$$

the following relation is applicable

$$v = -K^* \cdot |\nabla P|^{-0.5} \cdot \nabla P \quad (3)$$

where

$$K^* = 4 \cdot \frac{\sqrt{a_h}}{\sqrt{g \cdot \rho}} \cdot \log \left[ \frac{3.7}{k/D_h} \right]$$

and  $a_h$ ,  $g$  are the fracture aperture and the gravity constant. The Louis law can be obtained from the Nikuradse law by replacing the constant "3.7" in equation 4 by "1.9".

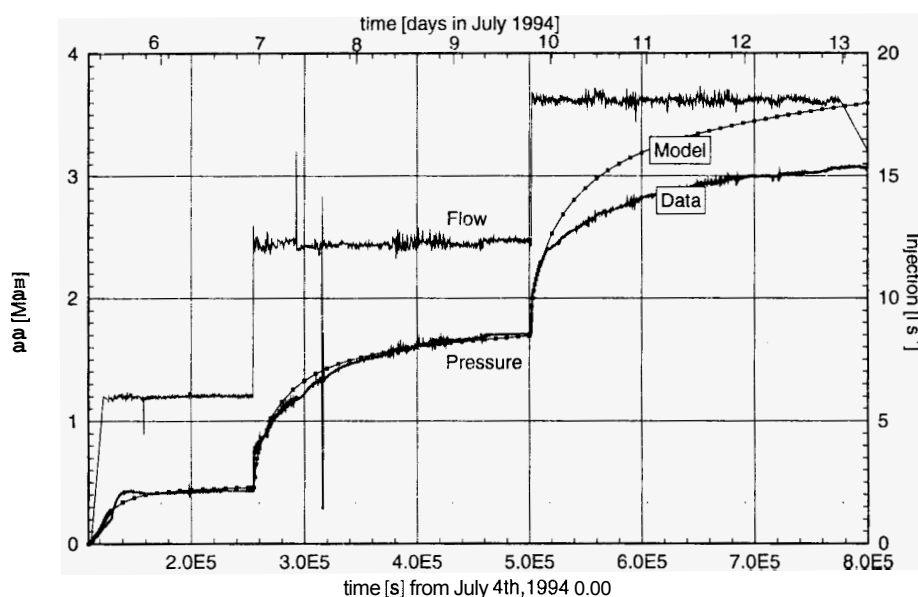


Figure 2: Record of flow rate (stable-steps) and downhole differential pressure during the injection test. Time is given in seconds on the lower x-axis and in days on the upper x-axis. The best-fit model prediction for a fracture of length of 1000 m and a height of 50 m are shown by the circled line (see Table 1 for other parameters).

## 2D Model

It was intended to set-up a model that explains the dataset 94JUL04 by the smallest number of degrees of freedom. Thus, only three different material sets were chosen: borehole, fracture and bulk rock (Fig. 3). We shall refer to this fracture as conduit. The single-wing conduit is supposed to have a rectangular vertical shape of height,  $h$ , which connects the borehole to a fault. The bulk rock is taken to be uniform and described by an permeability and specific storage coefficient. Since the bulk rock is described by a continuum, 'equivalent porous medium' approach, it includes the effect of other fractures present within the medium. It was supposed that 60% of the total flow rate enters the formation over depth range of 50 m. However we consider the height of the fracture to be a variable in recognition of the possibility of vertical spreading or narrowing of the flow field within the formation. In the present study we assume the fault to have a sufficiently large capacity that it acts as a constant potential drain. The existence of such faults within the reservoir has been proposed by Jung (1992a) based on the analysis of other hydraulic tests conducted at various levels within GPK1. The usage of a vertical conduit is justified on geological grounds, and by the strong stress anisotropy present within the reservoir which favours flow within sub-vertical fractures striking approximately north-south (e.g. Heinemann-Glutsch, 1994; Jupe et al., 1993). We further assume that flow within the fracture is linear, and governed by the Nikuradse fully-turbulent flow laws. This is justified by the quadratic relationship between the steady-state AP and Q data pairs obtained from the 1994 tests (Jung et al., 1995).

The two empirical flow laws of Nikuradse and of Louis have been examined. The fracture is assumed to be rigid and its mean aperture is taken as a variable to be constrained. Since pressures remained 5-10 MPa below the jacking pressure during the test series, changes in fracture aperture in response to the pressure changes are likely to be small, although perhaps not insignificant, particularly at the highest injection pressure. Future studies will include the effects of fracture compliance. The coefficient of specific storage for flow within the conduit,  $S_s^c$ , is taken as the compressibility of the fluid, although the results are found to be insensitive to this parameter.

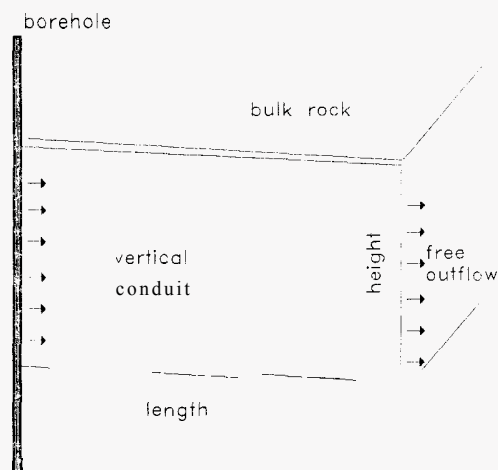


Figure 3: Schematic diagram of the model geometry. Flow enters the conduit from the borehole on the left and sweeps linearly across the conduit. The flow that has not leaked-off into the bulk rock exits into a constant-potential fault at the right.

A crucial role in the curve fitting is played by the transport properties of the bulk rock since it governs the long-term (hours to days) transient pressure response. We adopt an equivalent porous medium permeability of the bulk rock of  $3 \times 10^{-16} \text{ m}^2$ . Rummel (1992) reports matrix permeability values in the range of  $10^{-16}$  -  $10^{-18} \text{ m}^2$ , derived from laboratory tests on intact core samples. These values probably over-estimate in-situ matrix permeabilities due to thermal and stress relief micro-cracking. On the other hand, the bulk permeability most probably is increased by macro-scale, second order fractures. If we assume that on average each square metre of the wall of the conduit contains a 1 m long permeable fracture then our chosen bulk rock permeability corresponds to a hydraulic (equivalent parallel plate) aperture of  $15 \mu\text{m}$ . The

coefficient of specific storage for the bulk rock,  $S_s^r$ , is taken as a variable to be constrained by the curve fitting.

Since the problem is non unique, a liability study that was based on the property range was performed. Our purpose was that non-laminar analysis may lead to a restriction to those models with reliable properties of all parameters that are necessary for a description of the hydraulic field.

A series of models were run in which the prescribed variables were fracture length and height. For simplicity reasons, the hydraulic aperture of the fracture was taken to be the mean aperture of the fracture,  $\langle a \rangle$ . In the simulation process, the fracture apertures were obtained from steady state runs by fitting the long-term (steady-state) AP level. In a next step, the inversion procedure used these apertures in order to find the appropriate storage coefficient  $S_s^c$  by fitting the transient response to step increases in Q. Since FRACTure allows to define time-flow functions, the model's injection followed exactly the injection steps of the 94JUL04 dataset. Thus, it was ensured that the pressure history after each flow step was preserved.

## Results

The results of the fitting procedure are illustrated in Figure 2 for the case of a 1000 m long fracture of height 50 m. Note that in fitting the AP curve we have largely disregarded the long-term trend observed for the  $18 \text{ l s}^{-1}$  injection stage. To satisfactorily model this stage requires a more complex model than we have applied. This is evident from the fact that the steady-state P versus Q data point defined by this injection stage lies below the curve predicted for a fully-turbulent model (Figure 1). It is of note that the pressure record for this stage shows a marked discontinuity of the initial transient climb which is suggestive of the abrupt onset of fracture dilation (Figure 2). However, other mechanisms such as bifurcation of the flow path, cannot be ruled out. Future work will address this issue. For the moment we concentrate on fitting the first two stages of the test.

A good fit of the model prediction to the observations was obtained for the first two injection levels, and also for the initial part of the third-level transient. In particular, the long term rise in pressure towards an asymptotic level is well predicted. Within the framework of the model this rise is primarily governed by leak-off into the matrix. Flow within the fracture is comparatively quickly established, and thus influences only the initial steep rise in the transient. Since the leak-off flux is dependent upon the lateral pressure gradient prevailing in the walls of the fracture, it will decline with time as the pressure front penetrates the matrix. Thus, simple mass balance considerations require that fluid velocity within the fracture increase with time. It is this that accounts for the slow rise in pressure.

Clearly, the matrix transport properties and the net area of the fracture exert a major influence on the net leak-off, although the dependence on net area is not simple since the flow-law within the fracture is non-linear. Nonetheless, by requiring that the values of the matrix transport properties required to fit the data fall within reasonable physical bounds, useful constraints on fracture area can be obtained. The results of the curve-fitting procedure applied to different fractures of various heights and lengths are tabulated in Table 1. All models listed yield fits to the data which are similar to the model predictions plotted in Figure 2. The value of tile fracture specific storage coefficient is not listed since it did not significantly influence the results. Fracture length was varied between 100 m and 1000 m, and height between 5 and 200 m. Physically reasonable values for hydraulic aperture were obtained in all cases. However, only models which have a comparatively large swept area yield acceptable values for the matrix specific storage coefficient. If the crystalline rock through which leak-off occurs is considered free of open, compliant natural fractures, then we would expect  $S_s^r$  values of the order of  $10^{-11} \text{ Pa}^{-1}$  (Evans et al., 1992, p 105). However, in recognition of the presence of natural fractures, and the fact that the zone in question has been subjected to a major stimulation injection, we increase this by a factor of 50. Thus, the criterion for acceptable models is that  $S_s^r < 5 \times 10^{-10} \text{ Pa}^{-1}$ . Table 1 shows that this is satisfied by models with a fracture length of 1000 m and heights larger than 10 m. The minimum length which yields a satisfactory value for  $S_s^r$  is 200 m, although only for fracture heights which are somewhat larger than 200 m. Thus, comparatively large fracture surface areas are required to fit the data if the bulk rock permeability is less than  $3 \times 10^{-16} \text{ m}^2$ . Higher values of permeability could conceivably lead

to significant reductions in the required surface area, but are considered doubtful since  $3 \times 10^{-16} \text{ m}^2$  is an order of magnitude higher than the in-situ bulk-rock permeabilities measured in the GPK1 (Jung 1992b, Jung et al. 1995). Stimulation processes, such as shear-induced dilatation associated with microseisms, could be effective in increasing the bulk-rock permeability within a large volume. However, as noted earlier, to exceed  $3 \times 10^{-16} \text{ m}^2$  requires both a high density of stimulated conductive cross-cutting fractures and a high degree of stimulation (i.e. 15  $\mu\text{m}$  of dilation).

## Conclusions

Within the framework of the model, the results show that the transient response to the test injections can be explained by leak-off from a fracture of substantial surface area in which fully-turbulent flow is occurring. The increase in the duration of the transient with higher injection rates is predicted by the model and appears to demand non-laminar flow, at least if the fracture aperture remains essentially constant. Given the nature of the assumptions inherent in the model, we conclude that the results argue against a model in which the fluid exiting the borehole over the 50 m section below the casing shoe flows to a constant-potential fault through a short, channel-like flow path.

Future modelling must address the question of whether a series of sub-parallel fracture flow paths, each of which is substantially shorter, or a higher bulk rock permeability can also explain the data. A basic restriction to the present 2D model is the neglect of the three-dimensional nature of hydraulic diffusion into the bulk rock. This will have a reducing effect on the storage coefficient of the bulk rock and is especially of importance for the case of multiple, sub-parallel flow paths, that possibly have a minor height. Furthermore, the assumption of the existence of a constant-potential feature which collects the flow has to be investigated.

Table 1 Specified fracture dimensions and the parameter values required to give a satisfactory fit to the data

Length [m]	Height [m]	Aperture [mm]	$S'_s$ [Pa <sup>-1</sup> ]
1000	100	0.23	$5.0 \times 10^{-11}$
1000	50	0.37	$1.0 \times 10^{-10}$
1000	10	1.13	$5.0 \times 10^{-10}$
1000	5	1.83	$1.0 \times 10^{-09}$
200	200	0.075	$1.0 \times 10^{-09}$
100	100	0.105	$5.0 \times 10^{-09}$
100	50	0.17	$1.0 \times 10^{-08}$
100	10	0.53	$5.0 \times 10^{-08}$
100	5	0.85	$1.0 \times 10^{-07}$

## Acknowledgement

The authors would like to thank the Swiss "Bundesamt für Bildung und Wissenschaft" (BBW) for generously supporting this project. We also thank SOCOMINE for supervising the field experiments. The constructive comments of the reviewer are also gratefully acknowledged that helped to improve the manuscript.

Contribution No. 852, Institute of Geophysics, ETH-Zurich

## References

- Bruel D. & S. Ezzedine (1994), Etude des Phenomenes hydrauliques mécaniques et géochimiques dans les roches compactes fissurées au moyen de modèles à fractures discrètes, Internal Report, ADEME, Ecole des Mines, Paris, LHM/RD/93/05
- Cinco H.L. & F.V. Samaniego (1981). Transient Pressure Analysis for Fractured Wells, *J. Petrol. Tech.*, pp 1749-1766
- Evans K.F., T. Kohl, R.J. Hopkirk & L. Rybach (1992). Modelling of Energy Production from Hot Dry Rock Systems, Nationaler Energieforschungs-Fonds, Basel Switzerland, Final Report, pp 49-54
- Heinemann-Glutsch B. (1994), Results of scientific investigations at the HDR test site, Soultz-sous-Forêts, Alsace, Report prepared for Socomine, BP 39, route de Kutzenhausen, F-67250 Soultz s.F.
- Jung R. (1990). Hydraulic Fracturing and Hydraulic Testing in the Granitic Section of Borehole GPK1, Soultz s.F., Bundesanstalt für Geowissenschaften und Rohstoffe Hannover, BGR Report No 106616
- Jung R. (1992a), Hydraulic fracturing and hydraulic testing in the granitic section of the GPK1 borehole, in Soultz sous Forêts, Geothermal Energy in Europe - The Soutz Hot Dry Rock Project, Ed. J.C. Bresee, Gordon and Breach Science Publishers, Montreux, Switzerland, 149-198, 1992a.
- Jung R. (1992b), Connecting a borehole to a nearby fault by means of hydraulic fracturing, *Trans. Geothermal Resources Council*, Vol 16, Annual Meeting, San Diego. California, 433-438.
- Jung R. & R. Schellschmidt (1994). Erschliessung permeabler Risszonen für die Gewinnung geothermischer Energie aus heissen Tiefengesteinen, Dt. Geothermische Vereinigung, Jahrestagung, Schwerin
- Jung R., J. Willis-Richards, J.D. Nicholls, A. Bertozzi & B. Heinemann (1995), Evaluation of Hydraulic Tests at Soultz s.F., European HDR Site, *this volume*
- Jupe A., J. Willis-Richards & J.D. Nicholls (1993), Review of HDR Projects, Report No. ETSU G 164-P1, prepared for the UK Department for Trade and Industry.
- Kohl T. (1992), Modellsimulation gekoppelter Vorgänge beim Wärmeentzug aus heissem Tiefengestein, PhD Thesis ETH Zurich, No 9802
- Kohl T., K.F. Evans, R.J. Hopkirk & L. Rybach (1992), Modelling of coupled hydraulic, thermal and mechanical processes in the stimulation of Hot Dry Rock reservoirs behaviour, *Int. Symposium on Fractured and Jointed Rock Masses*, Lake Tahoe, USA
- Kohl T. & R. Hopkirk (1995), The finite element program 'FRACTure' for the simulation of Hot Dry Rock reservoir behaviour, *Geothermics*, in press
- Lomize G.M. (1951). Water Flow in Fissured Rocks, (in Russian), Gosenergoizdat, Moskwa
- Louis C. (1967), Stromungsvorgänge in kluftigen Medien und ihre Wirkung auf die Standsicherheit von Bauwerken und Boschungen im Fels, PhD Thesis University of Karlsruhe, published in: Veröffentlichungen des Institutes für Bodenmechanik und Felsmechanik, No 30
- Rummel F. (1992), Physical properties of the rock in the granitic section of borehole GPK1, Soultz-sous-Forêts, Geothermal Energy in Europe - The Soutz Hot Dry Rock Project, Ed. J.C. Bresee, Gordon and Breach Science Publishers, Montreux, Switzerland, pp.199-216
- Sharp J.C. (1970), Fluid Flow Through Fissured Media, PhD-Thesis University of London (Imperial College of Science and Technology)
- Turcotte D.L. & G. Schubert (1982). Geodynamics - Application of Continuum Physics to Geological Problems, *J. Wiley & Sons*, New York, p.238